

Cambridge University Press

978-1-107-41349-8 - Materials Research Society Symposium Proceedings: Volume 494:  
Science and Technology of Magnetic Oxides

Editors: Michael F. Hundley, Janice H. Nickel, Ramamoorthy Ramesh and Yoshinori Tokura  
Excerpt

[More information](#)

---

**Part I**

**Materials Processing of  
Metallic Magnetic Oxides**

Cambridge University Press

978-1-107-41349-8 - Materials Research Society Symposium Proceedings: Volume 494:  
Science and Technology of Magnetic Oxides

Editors: Michael F. Hundley, Janice H. Nickel, Ramamoorthy Ramesh and Yoshinori Tokura  
Excerpt

[More information](#)

---

Cambridge University Press

978-1-107-41349-8 - Materials Research Society Symposium Proceedings: Volume 494:  
Science and Technology of Magnetic Oxides

Editors: Michael F. Hundley, Janice H. Nickel, Ramamoorthy Ramesh and Yoshinori Tokura

Excerpt

[More information](#)DRY AND WET ETCH PROCESSES FOR NiMnSb, LaCaMnO<sub>3</sub> AND RELATED MATERIALS

J. Hong\*, J. J. Wang\*, E. S. Lambers\*, J. A. Caballero\*, J. R. Childress\*, S. J. Pearton\*, K. H. Dahmen\*\*, S. Von Molnar\*\*\*, F. J. Cadieu\*\*\*\* and F. Sharifi\*\*\*\*\*

\*Department of Materials Science and Engineering, University of Florida, Gainesville, FL

\*\*Department of Chemistry/MARTECH, Florida State University, Tallahassee, FL

\*\*\*Department of Physics/MARTECH, Florida State University, Tallahassee, FL

\*\*\*\*Physics Department, Queens College of CUNY, Flushing, NY

\*\*\*\*\*Department of Physics, University of Florida, Gainesville, FL

## ABSTRACT

A variety of plasma etching chemistries were examined for patterning NiMnSb Heusler thin films and associated Al<sub>2</sub>O<sub>3</sub> barrier layers. Chemistries based on SF<sub>6</sub> and Cl<sub>2</sub> were all found to provide faster etch rates than pure Ar sputtering. In all cases the etch rates were strongly dependent on both the ion flux and ion energy. Selectivities of  $\geq 20$  for NiMnSb over Al<sub>2</sub>O<sub>3</sub> were obtained in SF<sub>6</sub>-based discharges, while selectivities  $\leq 5$  were typical in Cl<sub>2</sub> and CH<sub>4</sub>/H<sub>2</sub> plasma chemistries. Wet etch solutions of HF/H<sub>2</sub>O and HNO<sub>3</sub>/H<sub>2</sub>SO<sub>4</sub>/H<sub>2</sub>O were found to provide reaction-limited etching of NiMnSb that was either non-selective or selective, respectively, to Al<sub>2</sub>O<sub>3</sub>. In addition we have developed dry etch processes based on Cl<sub>2</sub>/Ar at high ion densities for patterning of LaCaMnO<sub>3</sub> (and SmCo permanent magnet biasing films) for magnetic sensor devices. Highly anisotropic features are produced in both materials, with smooth surface morphologies. In all cases, SiO<sub>2</sub> or other dielectric materials must be used for masking since photoresist does not retain its geometrical integrity upon exposure to the high ion density plasma.

## INTRODUCTION

Ferromagnetic thin films and multilayers are currently being used in various magnetic recording, magnetic sensor and non-volatile memory applications. Interest in these materials for microelectronic applications has increased dramatically since the discovery of giant magnetoresistance (GMR) in multilayers comprised of alternating ultrathin (10-50Å) ferromagnetic/noble metal layers[1] and more recently the study of La-manganite perovskite colossal magnetoresistive (CMR) materials.[2] The Heusler alloy NiMnSb is a strong candidate for useful half-metallic behavior, which shows metallic for one spin type and insulating (or semiconducting) for the other, due to its high Curie temperature (720K).[3] Recently, significant experimental effort has been expanded to deposit high-quality thin-films of NiMnSb for magnetoresistive applications.[4-6] The spin filtering effect of NiMnSb thin layers will be maximized when the current flows normal to the layer plane, either resistively or by tunneling through an oxide barrier such as Al<sub>2</sub>O<sub>3</sub>. On the other hand, La-manganite materials requires above magnetic fields of about 1 Tesla to achieve most sensitive field-induced resistivity transition. Thus the necessary bias field is too large to be produced by an electrical current within the device, as is done for typical low-field magnetoresistive sensors. Consequently it may be necessary to provide a fixed, built-in bias field within the device, from a hard magnet materials such as SmCo. The fabrication of small, high quality etched patterns is particularly important to the potential applications of all these materials. In this paper, we report on selective wet and dry etch processes for NiMnSb and Al<sub>2</sub>O<sub>3</sub> structures, and on the Cl<sub>2</sub>-based plasma etching of LaCaMnO<sub>3</sub> and SmCo.

## EXPERIMENT

5000Å-thick NiMnSb thin films were deposited by magnetron sputtering with 2.5mTorr of Ar pressure, 30W of rf power onto glass substrate at the temperature of 350°. [6] Al<sub>2</sub>O<sub>3</sub> films were deposited with 2.5mTorr Ar pressure and 140W of rf power onto Si wafer substrates held at room temperature. Thin films of La<sub>x</sub>Ca<sub>1-x</sub>MnO<sub>3</sub> with x=0.41 were prepared on MnO(001) and Al<sub>2</sub>O<sub>3</sub>(0001) single crystal substrates by liquid delivery metalorganic chemical vapor deposition (LD-MOCVD). The SmCo-based films were directly crystallized by RF diode sputtering (100mTorr Ar) onto moderately heated (375-425°C) polycrystalline aluminum oxide substrates. The samples had a nominal composition of Sm 13%, Co 58%, Fe 20%, Cu 7%, Zr 2% and were directly crystallized upon deposition into the disordered TbCu<sub>7</sub> type crystal structure.

The samples were masked with either photoresist, SiN<sub>x</sub>, SiO<sub>2</sub> or apezon wax for etching experiments. Dry etching was performed in a Plasma Therm SLR 770 system. [7] The plasma is generated in a low profile Astex 4400 Electron Cyclotron Resonance (ECR) source operating at 2.45GHz and input powers from 0-1000W. The He back side cooled sample chuck is separately biased with 13.56MHz rf power from 50-450W, with induced dc self-bias of -90 to -1000V depending on the gas chemistry and microwave source power. Etch depths were obtained by stylus profilometry after removal of the mask materials in either acetone (photoresist) or trichloroethylene (wax). The etched surface morphologies were examined by Scanning Electron Microscopy (SEM) and Atomic Force Microscopy (AFM) in the tapping mode.

## RESULTS AND DISCUSSION

The sputter and etch rates for NiMnSb and Al<sub>2</sub>O<sub>3</sub> in ECR Ar, CH<sub>4</sub>/H<sub>2</sub>/Ar, Cl<sub>2</sub>/Ar discharges are shown in Figure 1, for a fixed rf chuck power (250W for Ar, CH<sub>4</sub>/H<sub>2</sub>/Ar and 150W for Cl<sub>2</sub>/Ar) and pressure (1.5mTorr), as a function of microwave source power. As this source power is increased, the ion density in the discharge is increased (from ~10<sup>9</sup> cm<sup>-3</sup> at 0W to ~3×10<sup>11</sup> cm<sup>-3</sup> at 1000W), and even though this suppresses the dc self-bias in the sample chuck (i.e. the acceleration potential for ions incident in the sample), the etch rates of both materials increase due to the higher ion flux. For microwave power source powers up to ~400W, there is no measurable sputtering of the Al<sub>2</sub>O<sub>3</sub>, and thus at lower powers the Al<sub>2</sub>O<sub>3</sub> can act as an etch stop when removing overlying NiMnSb films. In CH<sub>4</sub>/H<sub>2</sub>/Ar discharges under similar conditions of rf power, pressure and total gas flow rate, the etch rates of both materials are almost independent of microwave source power, and somewhat lower than with pure Ar. This may be due to shielding of the surface by polymer deposition at high source power, as is found for CH<sub>4</sub>/H<sub>2</sub>/Ar ECR etching of semiconductors. [7] Faster etch rates were obtained for both materials in Cl<sub>2</sub>/Ar discharges. The enhancement in NiMnSb etch rates relative to pure Ar under the same conditions ranged from ~10% at low microwave source powers to ~30% at 1000W, even at lower ion energies. The etch rates for NiMnSb were up to a factor of two higher than for Al<sub>2</sub>O<sub>3</sub> at high source powers. While etch products such as SbCl<sub>3</sub> and AlCl<sub>3</sub> are quite volatile, nickel and manganese chlorides have relatively low vapor pressures and require ion assistance to promote their desorption. The advantage of the high ion fluxes under ECR conditions is two-fold. [8] First, in strongly bonded materials such as Al<sub>2</sub>O<sub>3</sub>, one of the rate-limiting steps will be the ability to initially break bonds in order to allow the etch products to form. Therefore, at constant etch yield (i.e. atoms of the substrate removed per unit incident ion), a higher ion flux will produce a higher etch rate. The second advantage of the ECR discharges is that the high ion flux more effectively assists etch product desorption. Under more conventional reactive ion etching conditions this ion-assisted desorption is inefficient, allowing a thick selvedge or reaction layer of the involatile etch products to form on the sample surface. This layer shields

the surface from further interaction with the plasma and etching stops. The selectivity for etching NiMnSb over  $\text{Al}_2\text{O}_3$  is  $\leq 2$  in  $\text{Cl}_2/\text{Ar}$  over the microwave source power range 300-800W.

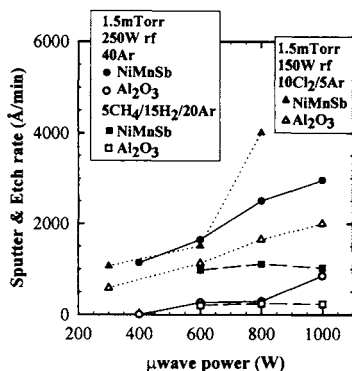


Figure 1. Etch rates of NiMnSb and  $\text{Al}_2\text{O}_3$  as a function of microwave source power in 1.5mTorr 250W rf chuck power discharges of Ar or  $\text{CH}_4/\text{H}_2/\text{Ar}$  and 150W rf chuck power discharges of  $\text{Cl}_2/\text{Ar}$ .

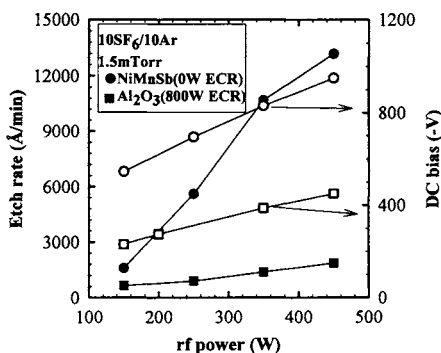


Figure 2. Etch rates of NiMnSb and  $\text{Al}_2\text{O}_3$  as a function of rf chuck power in 1.5mTorr discharges of  $\text{SF}_6/\text{Ar}$  at either 800W ( $\text{Al}_2\text{O}_3$ ) or 0W (NiMnSb) microwave source power.

The most efficient etching of NiMnSb was found with the  $\text{SF}_6/\text{Ar}$  plasma chemistry. In fact the etch rates were  $\geq 1.6\mu\text{m min}^{-1}$  even for the lowest microwave source power at which ECR discharges were stable, namely 400W. The etch rates were impossible to accurately quantify at high powers because the entire NiMnSb film disappeared in  $\leq 15$ secs under these conditions. By contrast, the etch rates of  $\text{Al}_2\text{O}_3$  are  $\leq 1200\text{Å min}^{-1}$  over the entire range of source powers, leading to selectivities of NiMnSb over  $\text{Al}_2\text{O}_3$  of  $\geq 20$ . This is not too surprising given that  $\text{AlF}_3$  is significantly less volatile than  $\text{AlCl}_3$ , reducing the etch rate of  $\text{Al}_2\text{O}_3$  in fluorine-based plasma chemistries relative to that in chlorine-based chemistries.

Besides ion flux, the other critical parameter in etching strongly bonded materials is ion energy.[8] This is controlled by the rf power applied to the sample chuck. At fixed microwave source power, the ion energy will be increased in a roughly linear fashion by increasing the chuck power.[9,10] Figure 2 shows the etch rates of both materials in  $\text{SF}_6/\text{Ar}$  discharges as a function of rf chuck power. In this case we used a relatively high microwave source power for  $\text{Al}_2\text{O}_3$  etching, but did not power the ECR source for the NiMnSb experiments because the rates were unmeasurably high as discussed earlier. At higher dc self-biases the etch rates are expected to increase because of more efficient bond breaking initially in the materials at higher incident ion energies, and the higher sputter yields of the etch products. Figure 3 shows the sputter rates in pure Ar discharges and etch rates in  $\text{Cl}_2/\text{Ar}$  discharges of  $\text{LaCaMnO}_3$  and  $\text{SmCo}$  as a function of rf chuck power. Note that the results for  $\text{Cl}_2/\text{Ar}$  basically follow those for pure sputtering (Ar), indicating that the La, Ca and Mn chlorides are not particularly volatile even at the high ion fluxes. As a comparison, there was a substantial degree of chemical enhancement observed for the etching of  $\text{SmCo}$  in  $\text{Cl}_2/\text{Ar}$  chemistries. The etch rate is approximately a factor of 10 to 12 higher than pure Ar up to dc self-biases of  $\sim 217\text{V}$ ; at higher biases the etch rate with  $\text{Cl}_2/\text{Ar}$  saturates and then decreases. Up to a particular ion energy, the etch rate is increased by the higher sputtering efficiency that more efficiently desorbs the etch products. However, above this

energy (in these experiments  $\sim 250\text{eV}$ ) the ions are able to desorb the chlorine radicals before they are able to react with the SmCo and hence the etch rates decreases.

Another important consideration is selection of a mask material for the etching process. Photoresist is typically not suitable for high density plasma processes because the high ion currents lead to reticulation.[11] Figure 4 shows  $\text{Cl}_2/\text{Ar}$  etch selectivity for both SmCo and LaCaMnO<sub>3</sub> over the dielectric SiO<sub>2</sub> and SiN<sub>x</sub>. Since there is basically no chemical enhancement for etching LaCaMnO<sub>3</sub>, there is also no selectivity over the dielectrics. This is a severe limitation if one needed to pattern deep features into LaCaMnO<sub>3</sub> because the mask thickness would need to be at least as thick as the required etch depth. For SmCo, however, the etch selectivity is  $\sim 4$  at low rf chuck powers and increases initially as this power is increased because the etch rate of the magnetic material rises faster than that of the dielectrics. At higher powers the selectivity decreases because of the fall-off in etch rate of the SmCo, and the fact that the dielectric etch rate continues to increase as ion energy is increased. Therefore, the modest chuck self-bias region is advantageous from the viewpoint of higher etch rates and selectivity with respect to the mask materials.

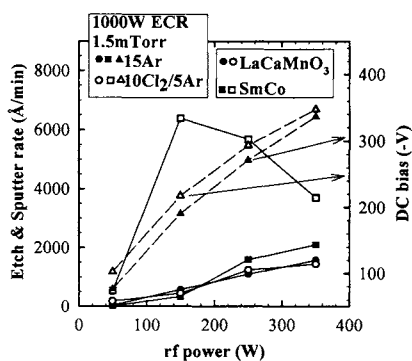


Figure 3. Etch rates of LaCaMnO<sub>3</sub> and SmCo in 1.5mTorr, 1000W microwave power discharges of pure Ar or Cl<sub>2</sub>/Ar as a function of rf chuck power.

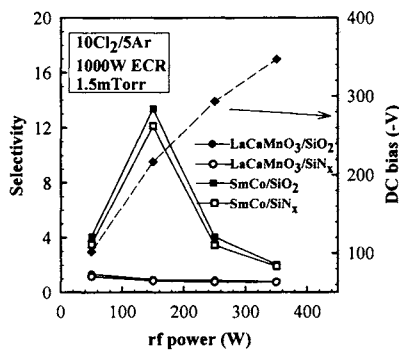


Figure 4. Selectivity for etching SmCo films or LaCaMnO<sub>3</sub> over either SiO<sub>2</sub> or SiN<sub>x</sub> mask materials, as a function of rf chuck power.

Both NiMnSb and Al<sub>2</sub>O<sub>3</sub> were found to exhibit a linear dependence of etch depth on time in HF/H<sub>2</sub>O solutions (Figure 5), and there was no measurable effect of solution agitation on etch rate. These are both characteristics of reaction-limited etching, where the critical parameter is temperature. Note in Figure 5 that the selectivity for NiMnSb is  $\sim 3:1$  over Al<sub>2</sub>O<sub>3</sub> based on the fact that the etch rates are equal at compositions of 1HF : 2H<sub>2</sub>O (NiMnSb) and pure HF (Al<sub>2</sub>O<sub>3</sub>). As mentioned previously an oxide forms readily on NiMnSb and thus HF solution would be expected to etch this material by removal of this oxide.

To obtain more highly selective etching of the NiMnSb, we examined the HNO<sub>3</sub> : H<sub>2</sub>SO<sub>4</sub> : H<sub>2</sub>O system at 25°C. The solution composition dependence of etch rates is shown in Figure 6. The etch rates of NiMnSb become extremely rapid as HNO<sub>3</sub> concentration is increased and thus dilution with H<sub>2</sub>SO<sub>4</sub> or H<sub>2</sub>O, or both, is necessary to achieve controllable rates (a few thousand angstroms per minute). The HNO<sub>3</sub> : H<sub>2</sub>SO<sub>4</sub> : H<sub>2</sub>O system is completely selective over Al<sub>2</sub>O<sub>3</sub> and thus thin layers of the latter can be employed as etch-stops. It is also desirable for practical applications to determine the nature of the etch reaction. Figure 7 shows an Arrhenius plot of the

NiMnSb etch rate in a 1:3 solution  $\text{HNO}_3 : \text{H}_2\text{SO}_4$ . The activation energy of  $16.7 \pm 3.4 \text{ kcal/mole}$  is typical of reaction-limited etching.[12] This is the preferred situation for obtaining reproducible pattern transfer, since the important parameter, namely temperature, can be well-controlled. If the etching is diffusion-limited, then the etch rate is dependent on solution agitation which is more difficult to reproduce, and moreover the etch depth proceeds as the square root of immersion time in the solution rather than the more straightforward linear dependence of reaction-limited etching.

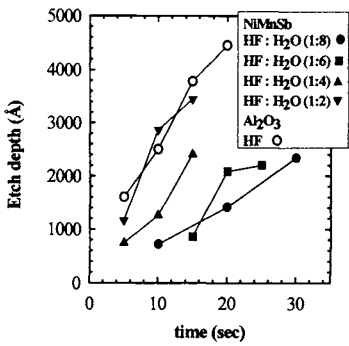


Figure 5. Etch depth versus time of NiMnSb and  $\text{Al}_2\text{O}_3$  in HF/ $\text{H}_2\text{O}$  solutions at  $25^\circ\text{C}$ .

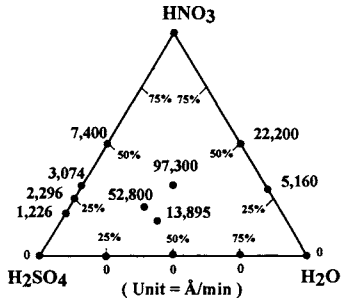


Figure 6. Etch rates (in  $\text{\AA}/\text{min}$ ) of NiMnSb as a function of solution formulation in  $\text{HNO}_3/\text{H}_2\text{SO}_4/\text{H}_2\text{O}$  at  $25^\circ\text{C}$ .

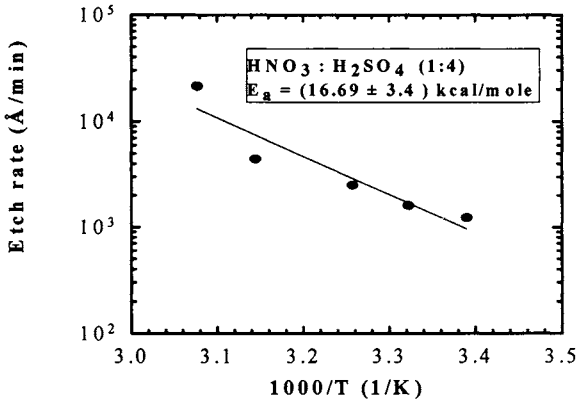


Figure 7. Arrhenius plot of NiMnSb etch rate in  $1\text{HNO}_3/3\text{H}_2\text{SO}_4$  solutions.

CONCLUSIONS

Several plasma chemistries ( $\text{Cl}_2/\text{Ar}$ ,  $\text{CH}_4/\text{H}_2/\text{Ar}$  and  $\text{SF}_6/\text{Ar}$ ) were investigated for the etching of NiMnSb/ $\text{Al}_2\text{O}_3$  structures under ECR conditions. The latter plasma chemistries

Cambridge University Press

978-1-107-41349-8 - Materials Research Society Symposium Proceedings: Volume 494:  
Science and Technology of Magnetic Oxides

Editors: Michael F. Hundley, Janice H. Nickel, Ramamoorthy Ramesh and Yoshinori Tokura

Excerpt

[More information](#)

produces the highest etch rates for NiMnSb and consequently the highest etch selectivity over  $\text{Al}_2\text{O}_3$ . Non-selective etching of both materials is obtained over a wide range of conditions in the other plasma chemistries. These processes will be useful in fabrication of small geometry spin-valve and GMR devices, especially at sub-micron dimensions. For larger area structures, pattern transfer can be obtained using two different wet etch processes, namely  $\text{HF}/\text{H}_2\text{O}$  for non-selective etching of NiMnSb/ $\text{Al}_2\text{O}_3$  and  $\text{HNO}_3/\text{H}_2\text{SO}_4/\text{H}_2\text{O}$  for selective etching of NiMnSb over  $\text{Al}_2\text{O}_3$ .

$\text{LaCaMnO}_3$  showed no chemical enhancement with  $\text{Cl}_2/\text{Ar}$  discharges due to the low volatilities of the potential etch products. For this material, therefore, simple Ar ion milling at modest acceleration voltages to avoid preferential sputtering effects is probably the best choice for pattern transfer processes. By contrast, chemical etch enhancements relative to pure Ar sputtering were obtained for SmCo with  $\text{Cl}_2/\text{Ar}$  over the whole range of dc self-biases examined. Selectivities as high as ~12 were obtained for SmCo with respect to  $\text{SiO}_2$  and  $\text{SiN}_x$  in  $\text{Cl}_2/\text{Ar}$  discharges.

#### ACKNOWLEDGEMENT

The work is supported by a DARPA grant monitored by S. Wolf, NON00014-961-0767, partially supported by a DOD MURI monitored by AFOSR (H. C. DeLong), contract F49620-96-1-0026, and by a subcontract through Honeywell (ONR grant N00014-96-C-2114).

#### REFERENCES

1. M. N. Baibich, J. M. Broto, A. Fert, F. Nguyen Van Dau, F. Petroff, P. Etienne, G. Creuzet, A. Friederich and J. Chazelas, *Phys. Rev. Lett.* **66**, 2472 (1988).
2. R. von Helmolt, J. Wecker, B. Holzapfel, L. Schultz and K. Samwer, *Phys. Rev. Lett.* **71**, 2331 (1993).
3. M. J. Otto, R. A. M. van Woerden, P. J. van der Valk, J. Wijngaard, C. F. van Bruggen, C. Hass, and K. H. J. Buschow, *J. Phys. : Condens. Matter* **1**, 2341 (1989).
4. J. S. Moodera, L.R. Kinder, T.M. Wong and R. Meservey, *Phys. Rev. Lett.* **74**, 3273 (1995).
5. J. F. Bobo, P. R. Johnson, M. Kautzky, F. B. Mancoff, E. Tuncel, R. L. White and B. M. Clemens, *J. Appl. Phys.*, **81** 4164 (1997).
6. J. A. Caballero, F. Petroff, Y. D. Park, A. Cabbibo, R. Morel and J. R. Childress, *J. Appl. Phys.* **81** 2740 (1997).
7. J. W. Lee, S. J. Pearton, C. J. Santana, J. R. Mileham, E. S. Lambers, C. R. Abernathy, F. Ren and W. S. Hobson, *J. Electrochem. Soc.* **143** 1093 (1996).
8. for a discussion of high density plasmas, see for example High Density Plasma Sources, ed. O. A. Popov (Noyes Publications, Park Ridge, NJ 1996), M. A. Lieberman and A. J. Lichtenburg, Principles of Plasma Discharges and Materials Processing (Wiley and Sons, NY 1994); J. Asmussen, *J. Vac. Sci. Technol. A* **7** 883 (1989).
9. F. F. Chen, Chapter 1 in High Density Plasma Sources, ed. O. A. Popov (Noyes Publications, Park Ridge NJ 1996).
10. R. J. Davis and E. D. Wolf, *J. Vac. Sci. Technol.* **B8** 1798 (1990).
11. J. W. Lee and S. J. Pearton, *Semicond. Sci. Technol.* **11** 812 (1996).
12. S. S. Tan and A. G. Milnes, *Solid State Electron* **38** 17 (1995).



Cambridge University Press

978-1-107-41349-8 - Materials Research Society Symposium Proceedings: Volume 494:  
Science and Technology of Magnetic Oxides

Editors: Michael F. Hundley, Janice H. Nickel, Ramamoorthy Ramesh and Yoshinori Tokura

Excerpt

[More information](#)

## EPITAXIAL GROWTH MECHANISM AND PHYSICAL PROPERTIES OF ULTRA THIN FILMS OF $\text{La}_{0.6}\text{Sr}_{0.4}\text{MnO}_3$

Yoshinori Konishi<sup>1</sup>, Masahiro Kasai<sup>1</sup>, Masashi Kawasaki<sup>1,2</sup>, and Yoshinori Tokura<sup>1,3</sup><sup>1</sup> Joint Research Center for Atom Technology (JRCAT), Tsukuba 305, Japan<sup>2</sup> Department of Innovative and Engineered Materials, Tokyo Inst. of Technology,  
Yokohama 226, Japan<sup>3</sup> Department of Applied Physics, The University of Tokyo, Tokyo 113, Japan

### ABSTRACT

Thin films of  $\text{La}_{1-x}\text{Sr}_x\text{MnO}_3$  ( $x=0.4$ ) were fabricated using pulsed laser deposition (PLD) methods. The surface morphology of the films was sensitively affected by oxygen pressure during deposition. At high oxygen pressure (~150 mTorr), randomly aligned grains were nucleated on the epitaxial film. When the pressure was reduced to 100 mTorr, the epitaxial film had very smooth surface. Under this condition, the thickness dependence of resistivity and magnetization were analyzed. Even 6 nm thick film showed ferromagnetic metallic behavior. The AFM images of ultra thin films deposited on wet-etched  $\text{SrTiO}_3$  showed atomically flat terraces and 0.4 nm steps. The film growth mode can be tuned to either layer by layer or step flow by the deposition temperature.

### INTRODUCTION

Perovskite-type oxides have such versatile properties as superconductivity, ferroelectricity, and colossal magnetoresistivity [1-5]. Epitaxial multilayers composed of these oxides should explore new functional devices. Actually, trilayer tunnel junctions [6], current injection transistors [7], and superlattices [8] having manganite thin films as one of the electroactive components have been fabricated to demonstrate its capability to be utilized in future electronics. However, the surface and interface structures have been neither understood nor controlled in an atomic scale as have been done in semiconducting devices. In order to elucidate novel phenomena and utilize them in devices, each oxide layer must have not only smooth surface but also physical properties as expected. It is of great importance for this purpose to understand and control the epitaxy dynamics on an atomic scale.

In this study, we optimized the epitaxial growth conditions for perovskite-type manganese oxides  $\text{La}_{1-x}\text{Sr}_x\text{MnO}_3$  ( $x=0.4$ ) and measured physical properties of ultra thin films. We have also investigated the epitaxial growth behaviors on wet-etched  $\text{SrTiO}_3$  substrates. These substrates enabled us to control the growth mode in an atomic scale.

### EXPERIMENT

Thin films were fabricated using high vacuum PLD apparatus with an ArF excimer laser (193 nm) [9]. Background pressure was typically  $2 \times 10^{-9}$  Torr. A sintered

pellet of  $\text{La}_{0.6}\text{Sr}_{0.4}\text{MnO}_3$  (LSMO) was used as a target. We used two types of (100)  $\text{SrTiO}_3$  (STO) single crystals for substrates. One is as-polished and the other is wet-etched substrates [10]. Oxygen pressure and substrate temperature were changed to optimize the epitaxial growth condition. After the deposition, films were slowly cooled down to room temperature in 760 Torr oxygen atmosphere for an hour. Magnetization of the films was measured using a superconducting quantum interference device (SQUID) magnetometer and resistivity was measured by conventional four probe method.

## RESULTS

The surface morphology and crystal orientation of the films were sensitively affected by oxygen pressure. Scanning electron microscope (SEM) pictures and reflection high energy electron diffraction (RHEED) patterns shown in Fig.1 clearly indicate the oxygen pressure dependence of the surface morphology of the films deposited on as-polished substrates. Under high oxygen pressure condition, randomly aligned grains were nucleated on the epitaxial film, resulting in RHEED pattern having both streaks from the underlying epitaxial film and rings associated with the grains. When the pressure was reduced to 100 mTorr, the epitaxial films had very smooth surface as indicated by fine streaks in RHEED pattern as well as SEM picture.

We now show the thickness dependence of resistivity and magnetization. The films are deposited at the optimum condition, i.e. 100 mTorr. The results are summarized in Fig.2. For the films thicker than 20 nm, the residual resistivity was as low as  $1-2 \times 10^{-4} \Omega\text{cm}$ , the Curie temperature ( $T_c$ ) reached 350 K and magnetization saturated at 590 emu/cc ( $3.5 \mu_B / \text{Mn atom}$ ). These values are comparable to those of single crystals. For the films thinner than 12 nm, the residual resistivity increased and saturated magnetization and  $T_c$  decreased as decreasing the film thickness. However, ferromagnetic metallic behavior was observed for a film as thin as 6 nm. The origin of the degraded ferromagnetic and metallic properties was not clear yet. The lattice constant of STO is 3.905 Å and longer than LSMO by 0.9%. Therefore, it is plausible that the tensile strain caused by the coherent growth at the interface induced the degraded properties. Fig.3 shows the  $\theta$ -2 $\theta$  X-ray diffraction peaks of the films. As can be seen, the lattice constant was reduced for thinner films. Although it was difficult to detect the peaks for the films thinner than 4 nm, this trend agrees with the tensile strain at the interface.

For further investigation of the growth dynamics, we have fabricated thin films on wet-etched STO substrates which have atomically flat terraces and 0.4 nm steps [10]. Fig.4 shows the AFM images of about 10 nm thick film. When the substrate temperature was 750 °C, the surface morphology was rather rough but each grain had same height (~0.4 nm) agreeing with the size of the unit cell. The original step structure on the substrate was preserved as shown in the line profile. When the substrate temperature was increased to 820 °C, atomically smooth terraces and 0.4 nm steps were seen on the film. This fact clearly indicates the latter film grew in a step flow mode [11]. We illustrate the epitaxial growth of manganite thin film as shown in Fig.5. At relatively low substrate temperature, the migrating atoms on the terraces do not have enough kinetic energy to